



Impacts of the source temperature and its distance on the statistical behavior of the convective air turbulence

Ebrahim Mohammadi Razi^{1,2} · Saifollah Rasouli^{2,3}

Received: 23 June 2018 / Accepted: 30 August 2019 / Published online: 7 September 2019
© Springer-Verlag GmbH Germany, part of Springer Nature 2019

Abstract

In this paper, anisotropy and inhomogeneity of an indoor convective air turbulence are studied using two-channel moiré deflectometry by statistical analyzing of the angle of arrival (AA) fluctuations over about 1300 points on the wave front passing through the turbulent area. The beam of a laser source is expanded and collimated with a diameter of 18 cm by a telescopic system consisting of an aspheric lens and a telescope. This beam propagates horizontally through a turbulent area. A heater is used for generating a convection air turbulence. At the end of the turbulent medium, the distorted wave front enters the aperture of another telescope. By the aid of another telescopic system, the diameter of the beam is reduced to a value of 2 cm, and the beam enters to a two-channel moiré deflectometer. This device is able to measure AA of the wave front being fluctuated due to the turbulence. By statistical analyzing of the AA fluctuations in two perpendicular directions on the transverse plane, the homogeneity and isotropy of the turbulent medium are investigated at different distances from the heater in the presence of different temperature gradients. Results show that the temperature gradient and the distance from the heat source have considerable impacts on the inhomogeneity and anisotropy of the convective air turbulence. With increasing the distance from the heat source and decreasing the temperature gradient, the homogeneity increases, while by increasing the temperature gradient and in high distances from the heater, it becomes more isotropic. Finally, we report a way for estimating the depth of boundary layer.

Mathematics Subject Classification 00-01 · 99-00

1 Introduction

The atmospheric turbulence has garnered great deal of attraction in science and engineering, due to its various impacts in different fields such as astronomy, free space communications, navigation, adaptive optics, and atmospheric optics. The theory of turbulence is presented by

different models, among which the Kolmogorov's model is the most common one [1]. The other models including Tatarskii, Greenwood, Von Karman, and the modified Von-Karman model obey Kolmogorov in inertial range that based on the isotropy and homogeneity of the turbulence [1–3]. Over recent decades, many studies have shown that outdoor turbulence and indoor turbulence are not homogeneous and isotropic. Bertolotti et al. [4] created an indoor convective air turbulence using a horizontal heated Nichrome grid. They investigated the effects of the propagation distance and temperature gradient on the phase structure function (PSF) of the light beam propagating through a turbulent medium by interferometry method. The results showed that near the thermal source due to the anisotropy and inhomogeneity of the convective turbulence, PSF does not obey the Kolmogorov model. Consortini et al. [5] reported the anisotropy of near-ground turbulence. In their research, they measured the refractive structure function by a method based on measuring the relative dancing of two or more parallel

✉ Ebrahim Mohammadi Razi
e.mohammadi@ub.ac.ir

Saifollah Rasouli
rasouli@iasbs.ac.ir
https://iasbs.ac.ir/~rasouli/

¹ Department of Physics, Faculty of Basic sciences, University of Bojnord, P. O. Box: 1339, Bojnord, Iran

² Department of Physics, Institute of Advanced Studies in Basic Sciences (IASBS), P. O. Box: 45195-1159, Zanjan, Iran

³ Optics Research Center, Institute for Advanced Studies in Basic Sciences, P. O. Box: 45195-1159, Zanjan, Iran

beams, as a function of their mean distance. The beams propagate in two directions, parallel and perpendicular to the earth surface. Analysis of the structure function indicated that the optical scale of turbulence along the vertical direction is smaller than that in the horizontal direction. By comparison of AA variances along two directions in several experiments, Lukin showed that the atmospheric turbulence is anisotropic as light propagates through the medium in horizontal and vertical paths [6–9]. They also surveyed the effects of various atmospheric parameters such as temperature gradient and velocity gradient on the PSF [6]. By two probes installed horizontally and vertically to the earth surface, Biferale and Procaccia [10] showed that the atmospheric boundary layer turbulence exhibits a 3D statistical turbulence intermingled with flow patterns whose statistics has a quasi 2D nature. Through measuring of the AA fluctuations over an 11.8 km urban path, Du et al. [11] observed that the variance of the AA in vertical direction is more than horizontal. Rasouli and Rajabi [12] in a new setup using moiré deflectometry studied the inhomogeneity of ground-layer atmospheric turbulence during the day and night times. By comparing the structure function of AA in two directions and in two different distances from the earth surface, the authors found that the near-ground atmospheric turbulence is an inhomogeneous turbulence. In addition, the inhomogeneity coefficient is not constant in day and night times. Mohammadi Razi and Rasouli [13], using image motion monitoring method, investigated the inhomogeneity and anisotropy of near-ground turbulence. The light beams propagate through the medium at different heights from the earth surface. Analyzing the variances of AA fluctuations at end of path, the authors found that variances of AA in two directions as in two points at the same height are not equal. Wang et al. [14] measured the average intensity, the scintillation index, and the intensity correlation function for three beams which propagate at three different heights above the ground. Results reveal that along short links (210 m), only the intensity correlation function captures the anisotropic information of turbulence, corresponding to the refractive index anisotropy ellipse of the atmospheric fluctuations. Also many researchers reported evidences of anisotropy in the stratosphere [15–18]. Due to great difficulty in controlling all conditions in the atmospheric turbulence, the researchers attempted to produce the similar controlled condition of convective air turbulence, in the lab. The findings indicated that the convective air turbulence is an anisotropic and inhomogeneous medium [5, 19, 20]. A great deal of theoretical research has been made regarding the anisotropy. Researchers, adding the anisotropy term(s) to the power spectrum density investigated its (their) effect(s) to scintillation, beam spreading, and AA fluctuations [21–26]. Moreover, it has been

found that indoor turbulence and outdoor turbulence do not obey the Kolmogorov power spectrum density model [22, 27–34].

As mentioned above due to great difficulty in controlling all conditions in the atmospheric turbulence, recently, the authors used an electrical heater with a cross-sectional area of $50 \times 100 \text{ cm}^2$ to produce indoor convective air turbulence similar to the turbulence of the near-ground layers in laboratory and studied its homogeneity and isotropy in the presence of two-dimensional temperature gradients using the image motion monitoring method [20]. In that work, the homogeneity and isotropy of the turbulence have been investigated by comparing the statistical fluctuations of AA on four small areas of the wave front of the light beam passing through the convective air turbulent medium in two directions and for two distances from the heat source. In the work, only the statistics of the AA fluctuations in four regions of the wave front were investigated. Using the image motion monitoring with two or four subapertures in front of the telescope's aperture is a common method for characterizing the atmospheric turbulence features [35–39]. However, because of the limited number of the studied regions on the wave front, simultaneously investigating of the homogeneity and isotropy of the turbulence in the hole area of the wave front is not possible by this method. In this paper, the two-channel moiré-based deflectometry [40–44] is used to study the isotropy and homogeneity of the convective air turbulence by statistical analysis of the AA fluctuations in more than 1300 points. It is worth mentioning that using this setup, the statistical analysis of the AA fluctuations of the wave front is performed at a much larger area (the hole of the wave front) with much greater spatial resolution with respect to the four-image motion monitoring (imaging of four circular subapertures with a diameter of 3 cm [20]).

2 Experiment

Experimental works are done in the optics laboratory of the Institute for Advanced Studies in Basic Sciences (IASBS). The experimental setup used in this work includes a laser, an aspheric lens, two telescopes, an electrical heater, a two-channel moiré based deflectometry, a CCD camera, and a computer is shown schematically in Fig. 1. It is similar to that used in Ref. [20], but there is no mask with four subapertures in front of the second telescope, and in addition, a two-channel moiré based deflectometer for measuring the AA fluctuations is mounted behind the second telescope. The second harmonic of a continuous wave diode-pumped Nd:YAG laser beam is expanded by the aspheric lens and enters the first telescope (a 14 inch Celestron Schmidt–Cassegrain telescope). The telescope recollimates the beam with a diameter of 18 cm. The beam passes horizontally through

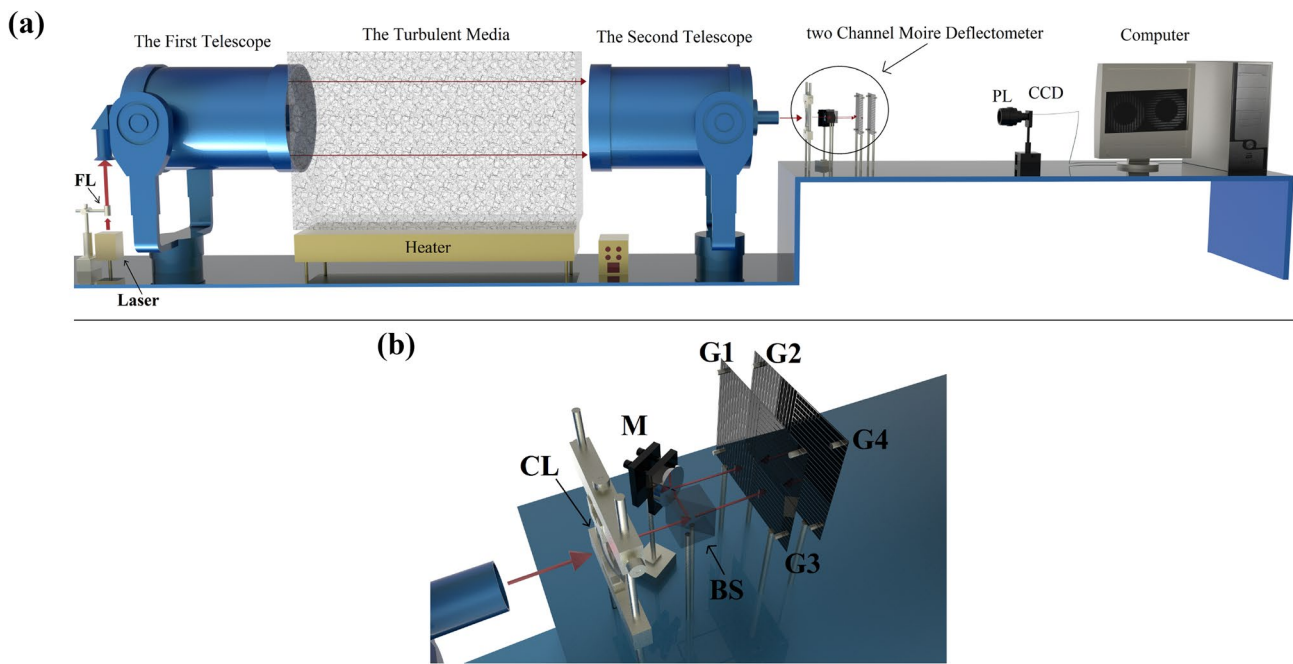


Fig. 1 Schematic diagram of the experimental setup: **a** a view from a far distance, and **b** a closed up view of the two-channel moiré deflectometry. FL, CL, BS, M, PL, and Gs stand for the focusing lens, collimating lens, beam splitter, mirror, the projecting lens, and gratings, respectively

an indoor air turbulence area. A flat plane heater with an upper surface area of $50 \times 100 \text{ cm}^2$ is installed under the light beam path to produce a vertical temperature gradient in the medium. Due to the limited width of heater's surface, a horizontal temperature gradient, TG, also arises. The magnitude of horizontal component of TG is directly affected by its vertical value and both are controlled by the heater's temperature. Using a set of temperature sensors, the values of two components of TG are approximately determined, and inequality of these two components can be revealed. The heater's altitude can be easily controlled using a jack being installed under it. At a specific height from the heater, temperature of the heater is adjusted from the room temperature to $100 \text{ }^\circ\text{C}$ with equal steps of $10 \text{ }^\circ\text{C}$. After passing through the turbulent area, the beam enters the second aperture (a 8 inch Meade LX200 GPS Schmidt–Cassegrain telescope). Two telescopes are installed at a distance of 150 cm. To investigate the isotropy and homogeneity of the turbulence in different distances from the heater, the two telescopes are installed at heights of 13, 30, 80, and 200 cm from the electrical heater's surface. The laser beam being collimated behind the second telescope's focal point by means of a collimator passes through a beam splitter, and then through a pair of moiré deflectometers being parallel and close together. The moiré patterns are formed on a plane where the second gratings of the moiré deflectometers are installed. The moiré patterns are projected on a CCD camera by a suitable lens and then transferred to a computer to be analyzed. The gratings' period and the Talbot distance

used in two-channel deflectometer are 0.1 mm and 37.5 mm, respectively. Data were recorded with a rate of 30 frames per second with an exposure time of 1 ms. In each experiment, 2000 images of moiré patterns were recorded.

It is worth mentioning that, in other experimental methods used for investigating anisotropy and inhomogeneity of the turbulence, the study area is small or at least the spatial resolution of the measurement is low, say about 1 cm. The use of two telescopes facing each other in conjunction with the use of a pair of moiré deflectometers provides high-resolution and high-precision measurements over a considerable large area. In the current work, we used two telescopes face-to-face and produced a plane wave with diameter of 18 cm. The AA fluctuation calculated with 0.2 arc sec precision over more than 1300 measurement points, simultaneously. To the best of our knowledge, the study of anisotropy and inhomogeneity of turbulence with such accuracy in measuring AA fluctuation and spatial resolution has been not performed so far. Also, the use of two telescopes face-to-face decreases the intrinsic divergence of the beam that is most important in a longer propagation path [12].

3 Theoretical consideration

Theoretical consideration of the AA calculation from two-channel moiré deflectometer is comprehensively discussed in Ref. [44]. Briefly, in the recorded moiré patterns, the trace of bright, dark, and the first virtual fringes from each

channel are determined. Points on horizontal traces match one by one to those of the vertical traces. Superimposing the horizontal traces onto the vertical one, the intersection of the traces is revealed to be an array of points. The intersection points are fluctuating due to the turbulence. Fig. 2a, b shows two arrays of the intersection points when the heater is off and when it is adjusted to 80 °C, respectively. The turbulence causes various displacements at different intersection points. For improving visualization, displacement vectors of the intersection points are plotted in Fig. 2c. As is apparent, the displacement vectors of the intersection points are bigger at lower altitudes, and vice versa.

One can calculate the AA fluctuations in two directions from the displacement values of the intersection points of a given sample frame with respect to the mean location of the intersection points as follows:

$$[\alpha_x, \alpha_y] = \frac{f'}{f} \frac{d}{z_k} \left[\frac{\Delta y_m}{d_m}, \frac{\Delta x_m}{d'_m} \right], \tag{1}$$

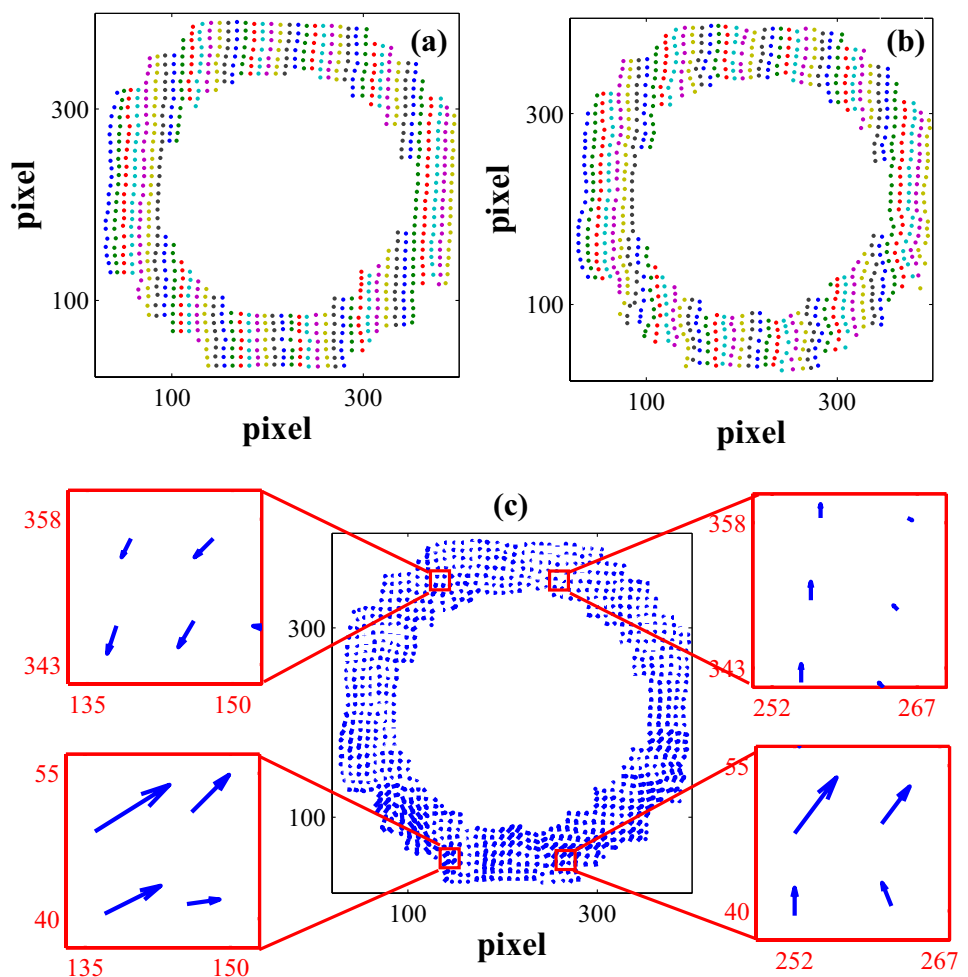
where $\alpha_{x(y)}$, f' , f , d , and z_k are the AA fluctuation in $x(y)$ direction, focal length of the second telescope, focal length

of the collimating lens, and k th Talbot distance, respectively. $\Delta y_m, \Delta x_m$ are moiré fringes shifts in the first and second channels (corresponding to the intersection point displacements in x - and y -directions), respectively, and d_m and d'_m are the moiré fringe spacings' in the first and second channels, respectively. By the aid of subpixel algorithm, the minimum measurable AA is determined by [44]

$$(\alpha_x)_{\min} = (\alpha_y)_{\min} = \frac{1}{MN} \frac{f'}{f} \frac{d}{z_k}, \tag{2}$$

where N is an integer number. If a minimum moiré fringe's shift with a value of $(\Delta x_m)_{\min} = (\Delta y_m)_{\min} = \frac{1 \text{ pixel}}{N}$ can be determined where N is an integer number, and if $d_m = d'_m$ and is covered by M pixels, according to the equipment's specifications say, $M = 26$ pixel, $N = 10$, $d = 0.1 \text{ mm}$, and $z_k = 37.5 \text{ mm}$, the minimum measurable AA fluctuation is determined equal to $(\alpha_x)_{\min} = (\alpha_y)_{\min} = 1.02 \times 10^{-6} \text{ rad} = 0.21 \text{ arc s}$.

Fig. 2 Illustration of the array of intersection points when **a** the heater is off and **b** the heater's temperature is 80 °C. **c** The displacements of the intersection points of **b** respect those of **a**. The insets show four enlarged parts of the displacement vectors' map. The light beam propagates at a height of 40 cm from the heater



4 Results and discussion

The effects of different temperature gradients and different distances from the heat source on the homogeneity and isotropy of the convective turbulence are investigated by calculating the AA fluctuations over the wave front at intersection points in two directions, parallel and perpendicular to the surface of the heater when the light beam passes at different heights of 13, 30, 80, and 200 cm from the heater surface and the temperature of heater’s surface changes from the room temperature to 100 °C by equal steps of 10 °C.

Figure 3 shows, for instance, the variance of the AA fluctuations in two directions at the intersection points of the wave front in front of the second telescope’s aperture at three selected heater’s temperature when the distance from the center of the light beam to the surface of the heater was 13 cm.

As is apparent, variance of each of the components of AA fluctuations increases as the heater temperature increases and also it increases when the distance from the heater decreases. The value of variance of AA fluctuations

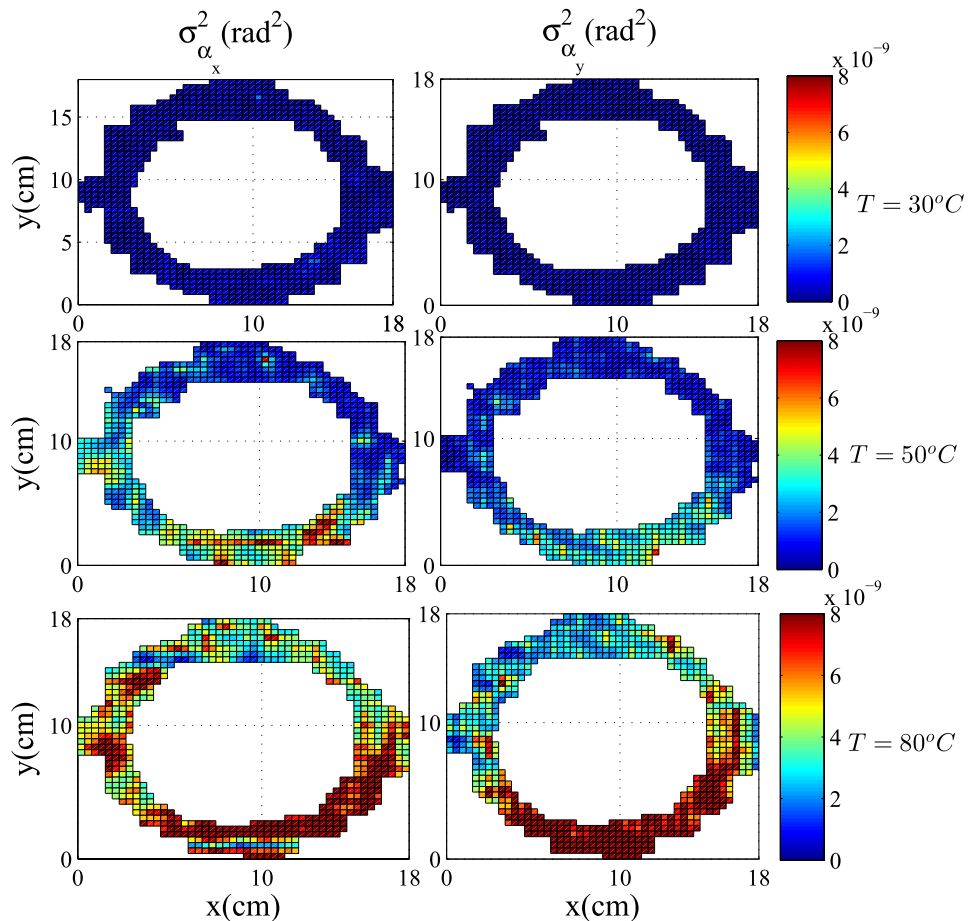
is directly related to the turbulence intensity, and thus, near the heater’s surface and at higher heater’s temperatures, the turbulence is more intense. This is in agreement with the results were reposted in the Ref. [20], but in that work, just the variance of AA fluctuations of four small regions of the wave front was calculated, while here, the number of studied points is more than 1300.

Figure 3 also reflects the effect of two-dimensional temperature gradient created by the heater on the homogeneity of the turbulence.

The variances of AA fluctuations along *x*- and *y*-directions do not differ, especially as the heater is off or its temperature is low. In other words, in these cases, the turbulence is almost homogeneous.

However, by increasing the temperature of the heater as well as approaching to the heater’s surface, a downward gradient for the variances of AA fluctuations appears. In other words, at large values of temperature gradient, the inhomogeneity is dominant behavior of the convective air turbulence. From comparison of the values of AA fluctuations in two directions in Fig. 3, existence of an anisotropy is quite clear. However for better illustration of the anisotropy of the convective air turbulence, and also to show the effects of the

Fig. 3 Variance of two components of the AA fluctuations at the intersection points for three heater’s temperatures. The light beam propagates at a height of 13 cm from the surface of the heater



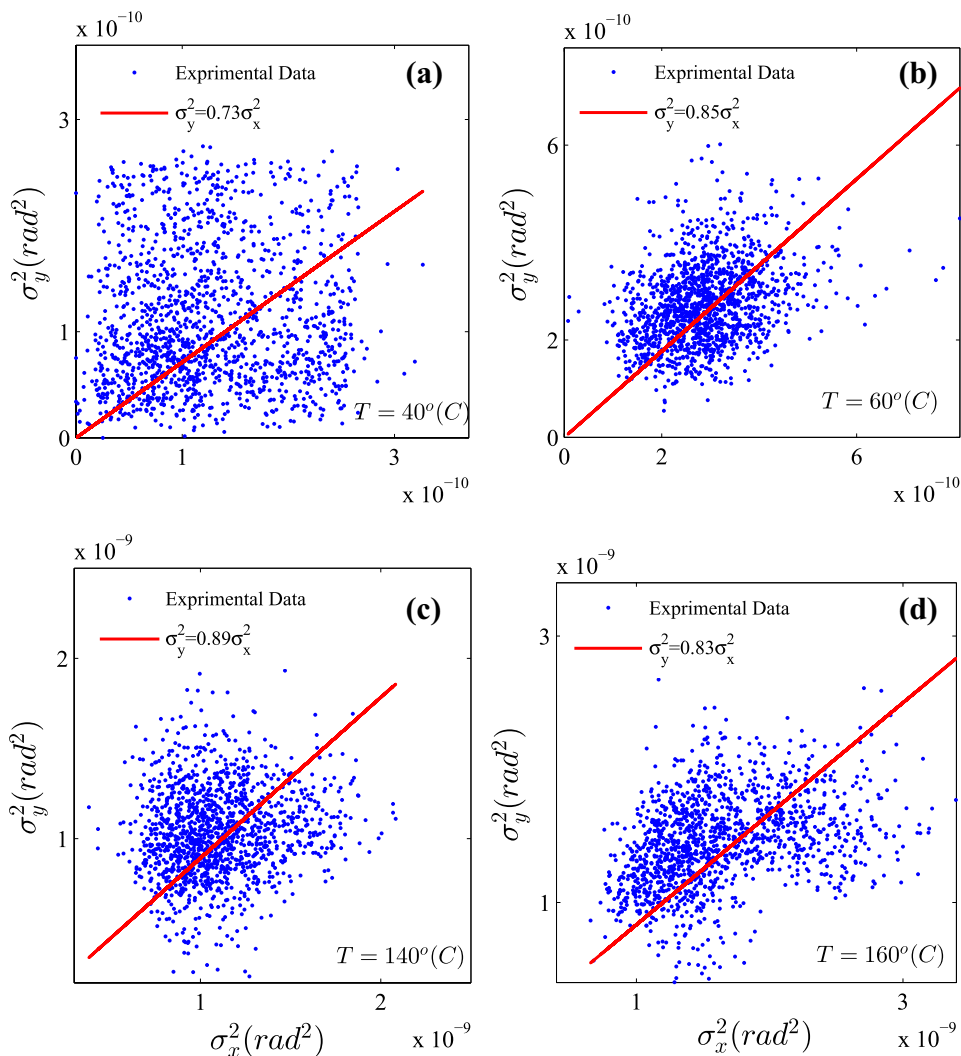
distance from the heat source and the different temperature gradient on the anisotropy, the variance of AA fluctuations in x direction is plotted versus that in the y direction for different distances of the light beam center from the heater surface as well as for different temperature gradients, see Fig. 4. For each set of data, a straight line is fitted to the experimental data. At the heater's surface temperatures of 40 °C, 60 °C, 140 °C, and 160 °C, corresponding values of $\frac{\sigma_y^2}{\sigma_x^2}$ are 0.73, 0.85, 0.89, and 0.83, respectively.

For investigating effect of the beam path distance from the heater surface, for each of the experiments, we calculate AA fluctuations over five horizontal regions on the wave front having different average altitudes. It means that we divide entire area of the wave front into five horizontal layers with different distances from the heater. In Fig. 5, fitted lines to the experimental data of y -component of variances of AA fluctuations versus x -component over five regions of wave front are shown for four experiments when the center of the light beam was at the heights of 13 cm, 30 cm, 80 cm, and

200 cm. The corresponding slopes of the fitted lines versus average height of the regions are plotted in the second row. All data were recorded with a heater temperature of 60 °C. It is seen that by increasing distance of the beam path from the heater surface, the value of $\frac{\sigma_y^2}{\sigma_x^2}$ increases except at the vicinity of the heater surface with values of h smaller than 10 cm.

Figure 6 shows the fitted lines to the experimental data of y -component of the variances of AA fluctuations versus x -component over the central region of the wave front at different temperature of the heater for four heights of the beam path from the heater surface: a 13 cm, b 30 cm, c 80 cm, and d 200 cm. Figure 6e–h shows the corresponding slopes of the fitted lines versus the heater's temperature. Here, we see that for a given height of the beam path from the heater surface, except $h = 13$ cm, by increasing the temperature of the heater, the slopes of the lines, say the value of $\frac{\sigma_y^2}{\sigma_x^2}$, increase. For the case $h = 13$ cm for the temperatures 30 °C and 40 °C, that behavior is violated.

Fig. 4 Fitted line to the experimental data of y -component of variances of AA fluctuations versus x -component in front of the second telescope's aperture at the heater's surface temperature of **a** 40 °C **b** 60 °C **c** 140 °C, and **d** 160 °C. The center of light beam was at a height of 80 cm from the heater's surface



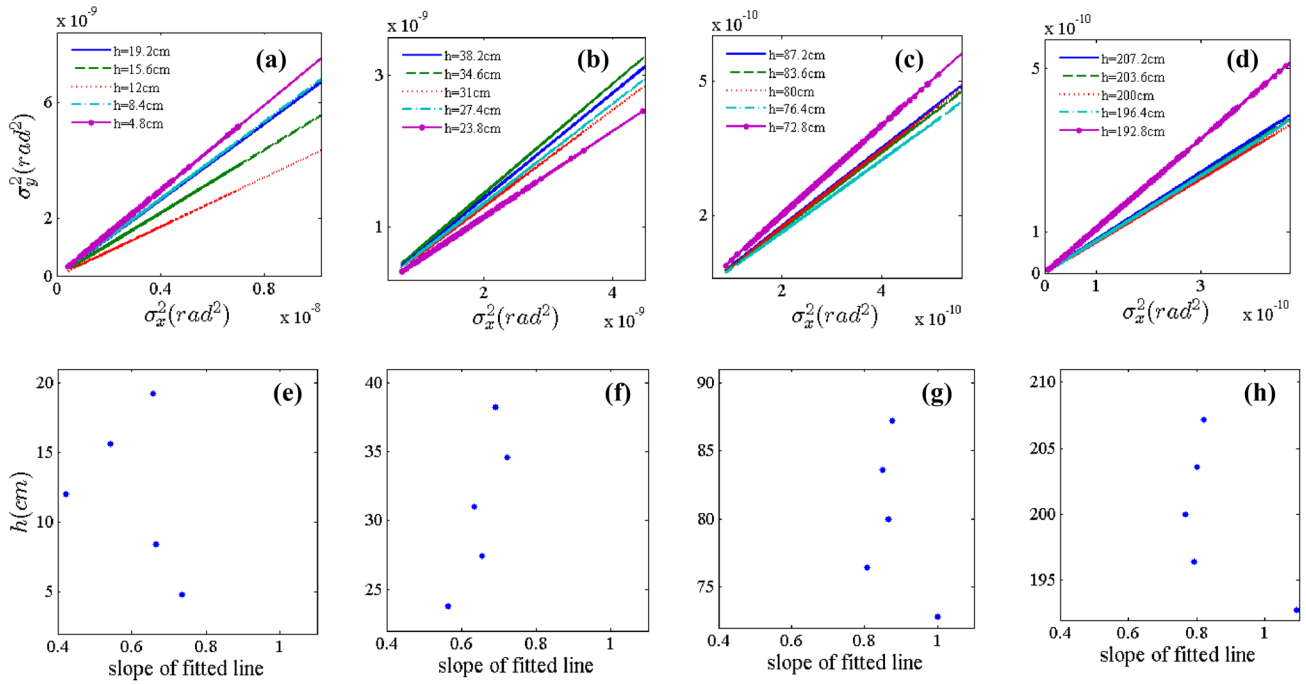


Fig. 5 Fitted lines to the experimental data of y -component of variances of AA fluctuations versus x -component over five regions of the wave front for four experiments when the center of the light beam

was at the heights of 13 cm, 30 cm, 80 cm, and 200 cm. The heater's temperature was 60 °C. The corresponding slopes of the fitted lines are plotted versus height in the second row

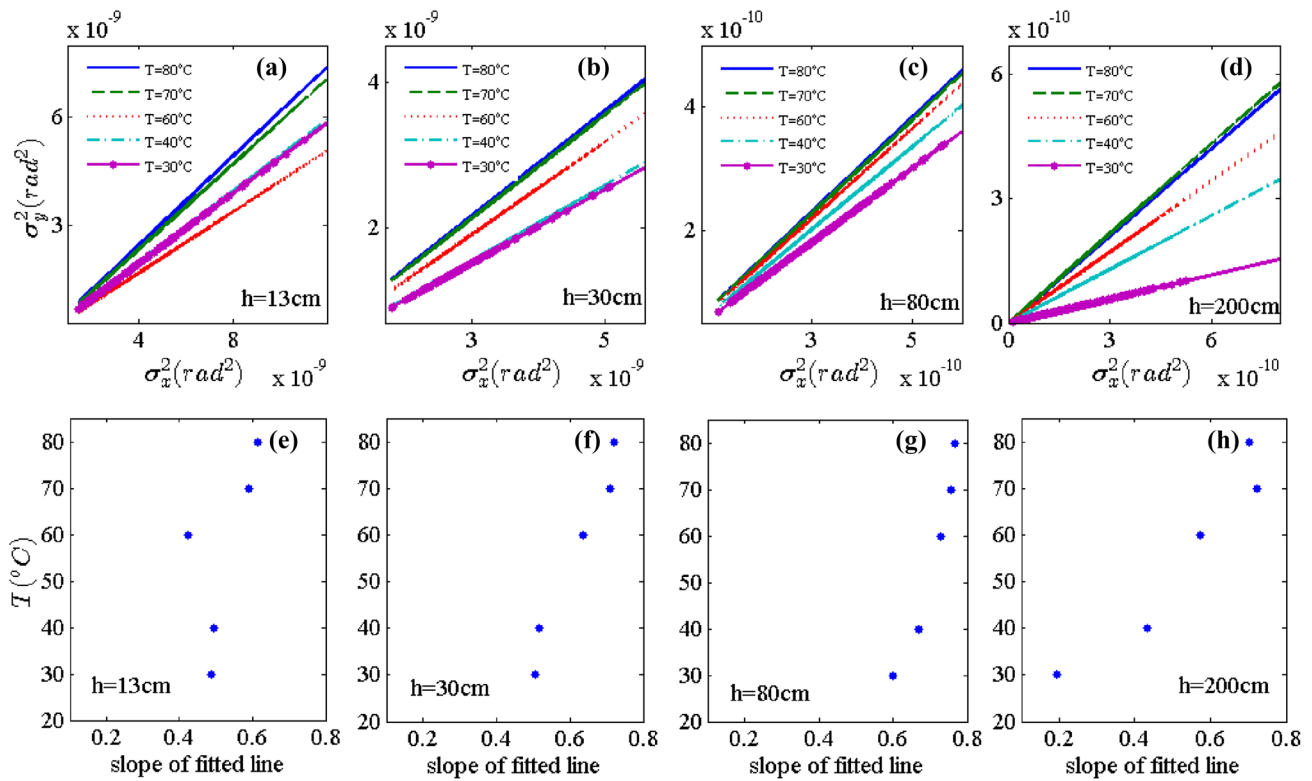


Fig. 6 Fitted lines to the experimental data of the ratio of two components of the variances of AA fluctuations over the central region of the wave front at different temperature of the heater for four heights

of the beam path from the heater surface: **a** 13 cm, **b** 30 cm, **c** 80 cm, and **d** 200 cm. **e–h** the corresponding slopes of fitted lines versus the heater's temperature

Figure 7 shows the data of the variance AA fluctuations in two directions for a situation that the light beam propagates through the turbulence medium in a height of 13 cm from the heater and the heater’s temperature was 70 °C. As is apparent, the turbulence behaves more isotropic at the height of 4.8 cm and then its isotropy decreases with increasing height up to the height of 12 cm and then the slope of the fitted lines re-increases for $h = 15.6$ cm and $h = 19.2$ cm. In this case, the height of boundary layer is revealed to be 12 cm. The height of the boundary layer is temperature-dependent and may be increase with heater’s temperature. Furthermore, from Fig. 7, it is clear that the turbulence is more

intense near the heater, since at the smaller heights, at the area close to the heater’s surface, the center of mass of the variance of AA data shifts to the right and upward sides. We think that the height of $h = 12$ cm having the smaller value of $\frac{\sigma_y^2}{\sigma_x^2}$ can be considered as the depth of the boundary layer.

Figure 8 shows the fitted lines to the experimental data of y -component of the variances of the AA fluctuations versus x -component over five regions of the wave front with different distances from heater’s surface for five values of the heater’s temperature: a 30 °C; b 40 °C; c 50 °C; d 60 °C; e 70 °C; and f 80 °C. In Fig. 8g–l, corresponding slopes of the fitted lines versus the height of the beam path from the heater’s surface.

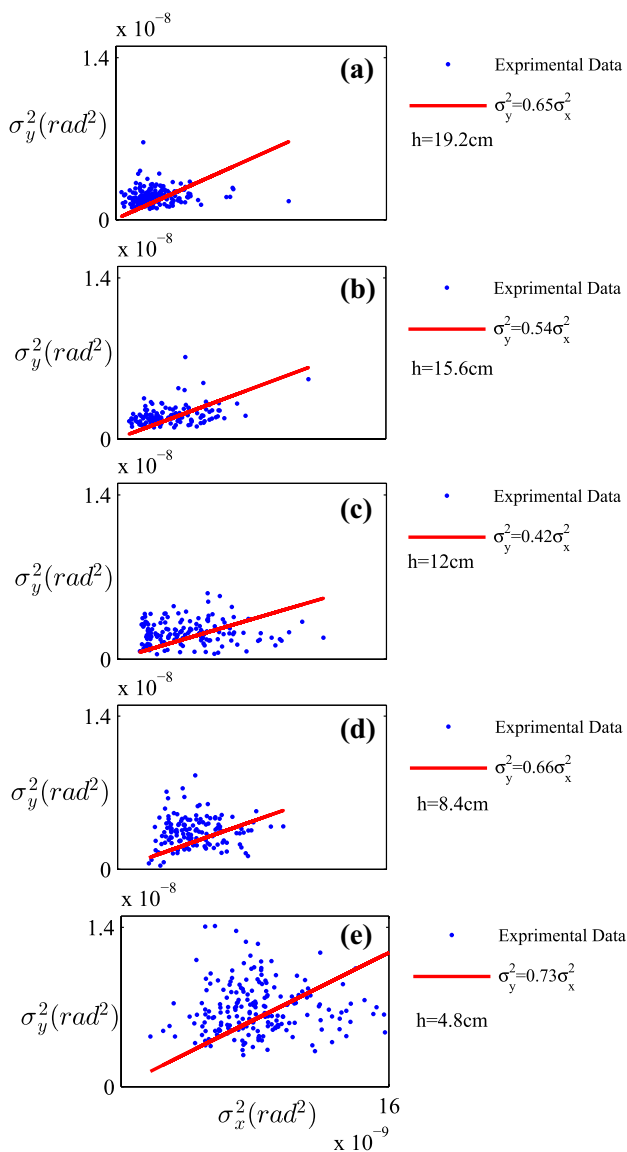


Fig. 7 Variances of the vertical component versus the horizontal one for the AA fluctuations in boundary layer. h is the average distance of the each region of the wave front from the heater surface. The heater’s temperature was 70 °C

5 Conclusion

Following our recent investigation on the homogeneity and isotropy of indoor convective air turbulence by analyzing of the statistics of the AA fluctuations in just four regions of the wave front via 4-apertures image motion monitoring method, in this research, the homogeneity and isotropy of the convective air turbulence were studied using statistics analysis of 1300 points on the wave front by a two-channel moiré-based deflectometry setup.

We show that the temperature gradient and distance from the heat source can effect on the inhomogeneity and anisotropy of the convective air turbulence. Our experimental results reflect that with increasing the distance from the heat source and decreasing the temperature gradient, the homogeneity increases and with increasing the temperature gradient in high altitudes, the isotropy of the turbulence increases. In addition, we presented a way for estimating of the depth of boundary layer.

Due to the complexity of the turbulence and the lack of a comprehensive theory for this phenomenon, we believe that our experimental findings, and also the presented high-resolution and wide area detection device might open a window to establish a more comprehensive theory for the phenomenon.

Finally, it is worth addressing to some potential applications of the presented work. However, further considerations are beyond the scope of the current work. The angle of arrival measured using two-channel deflectometry can be used to reconstruct the wave front of the light beam after being propagated through the turbulence medium. We have used this setup to investigate the effects of anisotropy and inhomogeneity of statistical variances of angle of arrival on the scaling of the phase structure function in indoor convective air turbulence, the results of which will be reported elsewhere [45]. In addition, the effects of anisotropy and inhomogeneity of the convective turbulence could be investigated

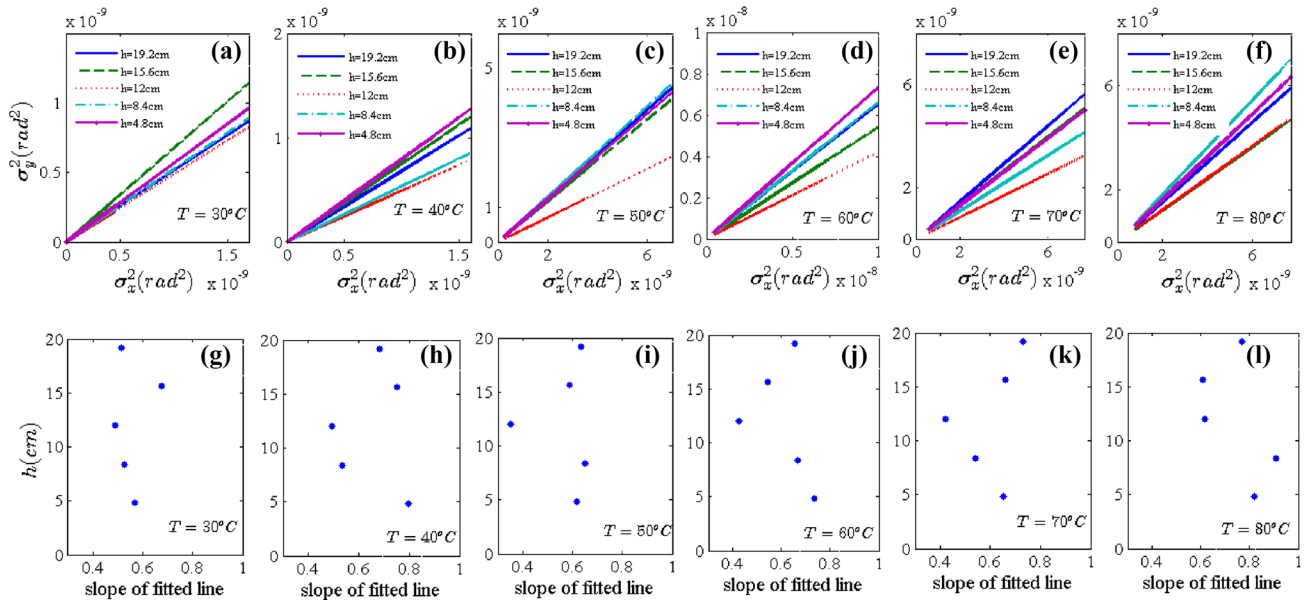


Fig. 8 Fitted lines to the experimental data of y-component of the variances of the AA fluctuations versus x-component over five regions of the wave front with different distances from heater’s surface for five values of the heater’s temperature: **a** 30 °C; **b** 40 °C; **c**

50 °C; **d** 60 °C; **e** 70 °C; and **f** 80 °C. **g–l** Corresponding slopes of the fitted lines versus the height of the beam path from the heater’s surface

on wave front aberrations and coherence function of the light beam. Results show that the coherence function and coherence length of turbulence were not equal in two directions perpendicular to the propagation direction.

References

1. L.C. Andrews, R.L. Phillips, *Laser Beam Propagation Through Random Media* (SPIE Press, Bellingham, 2005)
2. V.I. Tatarski, *Wave Propagation in a Turbulent Medium* (McGraw-Hill, New York, 1961)
3. D.P. Greenwood, D.O. Tarazan, Rome Air Development Center Griffiss AFB NY (No. RADCR-74-19) (1974)
4. M. Bertolotti, M. Carnevale, B. Crosignani, P. Di Porto, *Appl. Opt.* **8**(6), 1111 (1969)
5. A. Consortini, L. Ronchi, L. Stefanutti, *Appl. Opt.* **9**(11), 2543 (1970)
6. V.P. Lukin, V. Pokasov, *Appl. Opt.* **20**(1), 121 (1981)
7. V.P. Lukin, *Proc. SPIE* **2200**, 384 (1994)
8. V.P. Lukin, *Proc. SPIE* **2471**, 347 (1995)
9. V.P. Lukin, *Proc. IEEE* **1**, 22 (1996)
10. L. Biferl, I. Procaccia, *Phys. Rep.* **414**, 43 (2005)
11. W. Du, L. Tan, J. Ma, S. Yu, Y. Jiang, *Laser Part. Beams* **28**, 91 (2010)
12. S. Rasouli, Y. Rajabi, *Opt. Laser Technol.* **77**, 40 (2016)
13. E.M. Razi, S. Rasouli, *Opt. Commun.* **383**, 255 (2017)
14. F. Wang, I. Toselli, J. Li, O. Korotkova, *Opt. Lett.* **42**(6), 1129 (2017)
15. A.S. Gurvich, M.S. Belenii, *J. Opt. Soc. Am. A* **12**, 2517 (1995)
16. M.S. Belenkii, *Opt. Lett.* **20**, 1359 (1995)
17. A.S. Gurvich, I.P. Chunchuzov, *J. Geophys. Res.* **108**(D5), 6 (2003)

18. C. Robert, J.M. Conan, V. Michau, J.B. Renard, C. Robert, F. Dalaudier, *J. Opt. Soc. Am. A* **25**, 379 (2008)
19. A. Consortini, K.A. ODonnell, *Waves Random Media* **1**(3), S11 (1991)
20. E.M. Razi, S. Rasouli, *J. Opt.* **16**, 045705 (2014)
21. L. Cui, *Opt. Exp.* **23**(5), 6313 (2015)
22. I. Toselli, B. Agrawal, S. Restaino, *J. Opt. Soc. Am. A* **28**(3), 483 (2011)
23. V.S. Rao Gudimetla, R.B. Holmes, G. Smith, G. Needham, *J. Opt. Soc. Am. A* **29**(5), 832 (2012)
24. M. Yao, I. Toselli, O. Korotkova, *Opt. Exp.* **23**, 31608 (2014)
25. O. Korotkova, *Opt. Lett.* **40**, 3077 (2015)
26. I. Toselli, O. Korotkova, *J. Opt. Soc. Am. A* **32**(6), 1017 (2015)
27. L.C. Andrews, R.L. Phillips, R. Crabbs, T. Leclerc, *Proc. SPIE* **8874**, 887402 (2013)
28. D. Dayton, J. Gonglewski, B. Pierson, B. Spielbusch, *Opt. Lett.* **17**, 1737 (1992)
29. G. Funes, D. Gulich, L. Zunino, D.G. Prez, M. Garavaglia, *Opt. Commun.* **272**, 476 (2007)
30. V.E. Ostashev, D.K. Wilson, G.H. Goedecke, *J. Acoust. Soc. Am.* **115**, 120 (2004)
31. I. Toselli, L.C. Andrews, R.L. Phillips, V. Ferrero, *Proc. SPIE* **6457**, 64570T (2007)
32. I. Toselli, L.C. Andrews, R.L. Phillips, V. Ferrero, *Proc. SPIE* **6551**, 65510E (2007)
33. S. Gladysz, K. Stein, E. Sucher, D. Sprung, *Proc. SPIE* **8890**, 889013 (2013)
34. I. Arad, B. Dhruva, S. Kurien, V.S. L’vov, I. Procaccia, K.R. Sreenivasan, *Phys. Rev. Lett.* **81**, 5330 (1998)
35. D.L. Fried, *J. Opt. Soc. Am. A* **55**, 1427 (1965)
36. M. Sarazin, F. Roddier, *Astron. Astrophys.* **227**, 294 (1990)
37. A. Tokovinin, *Publ. Astron. Soc. Pac.* **114**, 1156 (2002)
38. A. Poisson, A. Fernandez, D.G. Perez, R. Barille, J.C. Dupont, *Opt. Laser Technol.* **80**, 33 (2016)
39. R. Shomali, S. Nasiri, A. Darudi, *J. Opt.* **13**, 055708 (2011)
40. S. Rasouli, M.T. Tavassoly, *Opt. Lett.* **31**, 3276 (2006)

41. S. Rasouli, M.T. Tavassoly, *Opt. Lett.* **33**, 980 (2008)
42. S. Rasouli, *Opt. Lett.* **35**, 1470 (2010)
43. S. Rasouli, M. Dashti, A.N. Ramaprakash, *Opt. Express* **18**, 23906 (2010)
44. M. Dashti, S. Rasouli, *J. Opt.* **14**, 095704 (2012)
45. S. Rasouli, E. Mohammadi Razi, J.J. Niemela, Investigation of the anisotropy and scaling of the phase structure function in convective air turbulence. **(to submitted)**

Publisher's Note Springer Nature remains neutral with regard to jurisdictional claims in published maps and institutional affiliations.